

## Topological Defects and Bulk Melting of Hexagonal Ice

Davide Donadio,\* Paolo Raiteri, and Michele Parrinello

Computational Science, Department of Chemistry and Applied Biosciences, ETH Zürich, USI Campus,  
Via Buffi 13, CH-6900 Lugano, Switzerland

Received: February 8, 2005

We use classical molecular dynamics combined with the recently developed metadynamics method [Laio, A.; Parrinello, M. *Proc. Natl. Acad. Sci. U.S.A.* **2002**, 99, 20] to study the process of bulk melting in hexagonal ice. Our simulations show that bulk melting is mediated by the formation of topological defects which preserve the coordination of the tetrahedral network. Such defects cluster to form a defective region involving about 50 molecules with a surprisingly long lifetime. The subsequent formation of coordination defects triggers the transition to the liquid state.

The melting of ice is a process of obvious universal relevance. Under ordinary circumstances melting is nucleated at surfaces,<sup>1,2</sup> but situations could be envisaged in which the effect of the surfaces is inhibited and melting becomes a bulk effect.<sup>3</sup> Studying melting under these circumstances can give very precious information on the nature of the potential energy surface (PES) and on the transition to the disordered state. One could in fact imagine that melting takes place either as a sudden collapse of the lattice or through the creation and successive catastrophic multiplication of defects.<sup>4</sup>

In principle, molecular dynamics (MD) is an ideal tool for studying bulk melting, since the imposed periodic boundary conditions eliminate surface effects. Unfortunately, the time scale over which melting occurs is too long for present-day computational resources. This means that melting can be observed only by superheating the system to the point of inducing a sudden lattice instability. Very recently, we have developed the metadynamics method, which allows long time scale phenomena to be studied.<sup>5–7</sup> Using metadynamics, we are able to study the melting of ice near the melting temperature of the adopted empirical model ( $\sim 270$  K), and we find that bulk melting is mediated by the formation of topological defects, named 5+7 and characterized in a recent work.<sup>8</sup> However, in contrast to the picture of a sudden multiplication of these defects, we find that, before melting, ice goes through a metastable state where a defective region of about 50 molecules is surrounded by an otherwise perfect lattice.

To overcome the time-scale problem, we exploit the extended Lagrangian implementation of metadynamics.<sup>6</sup> The method is based on the construction of a coarse-grained non-Markovian dynamics in the space defined by a few collective coordinates. The dynamics is biased by a history-dependent potential term that, in time, fills the free energy minima, allowing an efficient exploration and an accurate determination of the free energy surface (FES). As in ref 6, we introduce an extended Hamiltonian that couples the collective variables  $s_\alpha(\mathbf{r})$  to a set of

additional dynamic variables  $s_\alpha$

$$H = H_0 + \sum_{\alpha} \left[ \frac{1}{2} M_{\alpha} \left( \frac{ds_{\alpha}}{dt} \right)^2 + \frac{1}{2} k_{\alpha} (s_{\alpha} - s_{\alpha}(\mathbf{r}))^2 \right] + V(s_{\alpha}, t) \quad (1)$$

where  $\mathbf{r}$  is the microscopic coordinates of the system and  $H_0$  is the unperturbed Hamiltonian. The mass  $M_{\alpha}$  and the coupling constant  $k_{\alpha}$  should be chosen so as to achieve an efficient coupling between the microscopic system and the collective variables, which is obtained when the frequencies determined by  $M_{\alpha}$  and  $k_{\alpha}$  are of the same order of magnitude as the characteristic frequencies of the microscopic system. The history-dependent potential is defined as

$$V(s_{\alpha}, t) = \sum_{\substack{t_i = (\Delta t, 2\Delta t, \dots) \\ t_i < t}} w \exp \left( - \frac{||s_{\alpha} - s_{\alpha}(t_i)||^2}{2\delta s^2} \right) \quad (2)$$

where the time interval  $\Delta t$  between the placement of two successive Gaussians, the Gaussian width  $\delta s$  and the Gaussian height  $w$ , are free parameters that affect the efficiency and the accuracy of the algorithm.<sup>7</sup> This method has already been applied successfully to the study of rare events occurring in biological systems,<sup>9</sup> chemical reactions,<sup>10,11</sup> and phase transitions.<sup>12</sup>

Two different sets of collective variables were used in the study of the melting transition. Common to both sets is the use of the potential energy, which is a relevant order parameter for the melting as it undergoes a sizable change when the phase transition takes place. Moreover, it is suitable for use as a collective variable in the metadynamics scheme, as it is an explicit function of the microscopic configuration of the system.<sup>13</sup> The potential energy was supplemented by coordinates measuring the intermediate order. In one case, we exploited the Steinhardt<sup>14</sup> order parameter  $Q_6$ , which has already been used successfully to simulate the nucleation of ice  $I_h$  in liquid water,<sup>15</sup>

\* To whom correspondence should be addressed. E-mail: ddonadio@phys.chem.ethz.ch.

and in the other the number of five- and six-membered rings. In either case, we find similar results. Here we discuss only results obtained on the basis of the second choice.

To compute the ring statistics, we use the shortest path ring definition.<sup>16,17</sup> This is obtained by considering a H<sub>2</sub>O molecule and two of its nearest neighbors (n.n.) and finding the shortest closed path passing through these three molecules. This criterion fails when counting large primitive rings,<sup>17</sup> but these are of little importance for our study. For use in the metadynamics, it is necessary to turn this definition into a continuous differentiable function of the atomic coordinates  $\mathcal{N}_n(\{\mathbf{r}_i\})$  which gives the number of  $n$ -membered rings. We define the hydrogen bond between water molecules  $i$  and  $j$  by a function  $f_{ij}$  of the atomic coordinates, which is 1 when the two molecules are bonded and otherwise tends smoothly to zero.<sup>18,19</sup> For each H<sub>2</sub>O molecule, we consider the triplets  $T$  formed by itself and the pairs of its neighbors and we compute the products  $F_T^I = \prod_{i,j \in T} f_{ij}$  of the hydrogen bond functions in the closed paths  $I$  containing  $T$ . The shortest path ring containing  $T$  is selected by a function  $G_T$  defined as

$$G_T = \lambda / \ln \sum_{I \supset T} e^{\lambda F_T^I / L_I} \quad (3)$$

where  $L_I$  is the topological length of the path  $I$ . In the limit of large  $\lambda$ ,  $G_T$  tends to the length of the shortest path ring. The total number of  $n$ -membered rings is then given by a sum of rational functions

$$\mathcal{N}_n(\{\mathbf{r}_i\}) = \sum_T \frac{1 - \left( \frac{n - G_T}{\sigma} \right)^8}{1 - \left( \frac{n - G_T}{\sigma} \right)^{16}} \quad (4)$$

The parameters  $\sigma$  and  $\lambda$  are chosen so as to achieve the correct ring statistics while at the same time making the function  $\mathcal{N}_n(\{\mathbf{r}_i\})$  smooth enough to avoid problems in the integration of the equations of motion. In our calculation we have chosen  $\sigma = 0.3$  and  $\lambda = 150$ .

The initial proton-disordered configurations of ice were generated using the Monte Carlo procedure described in ref 20, which allows supercells with zero dipole moment to be produced. We employ the nonpolarizable TIP5P force field<sup>21</sup> and treat the long-range electrostatics exactly by the particle mesh Ewald algorithm. Although this model fails in reproducing the thermodynamics of water at high temperature ( $>500$  K),<sup>22</sup> the hydrogen bond dynamics,<sup>19</sup> the self-diffusion coefficient, and the density anomaly are well reproduced in the range of temperature of interest to this study ( $\sim 270$  K).<sup>21–23</sup> The melting of ice  $I_h$  was simulated in the constant pressure (NPT) ensemble in models consisting of 576 and 360 water molecules. No size effects on the results were observed while reducing the size of the system. The results reported below refer to simulations of a 576 molecule system. In these metadynamics runs the time-dependent potential (eq 2) is made up of Gaussians 0.5 kcal/mol high, placed every  $\Delta t = 1$  ps. The widths  $\delta s$  of the Gaussians in the space of the collective variables are 10 and 20 for five- and six-membered rings and 24 kcal/mol for the potential energy. This choice of parameters leads to an accuracy of  $\sim 1.5$  kcal/mol.

The evolution of the collective variables during the melting is reported in Figure 1. Before the phase transition takes place, a few events of formation and recombination of five-membered

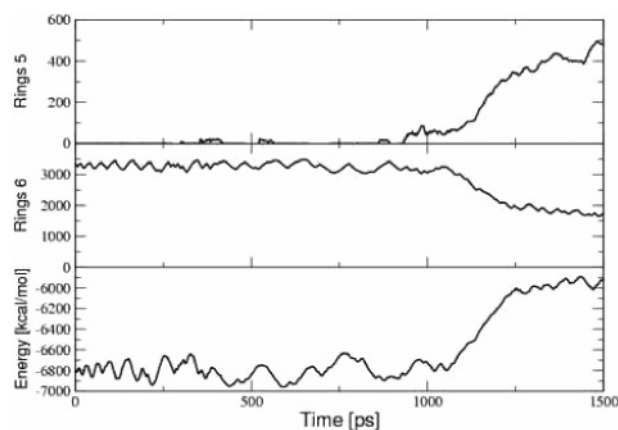


**Figure 1.** Evolution of the collective variables during a metadynamics trajectory for the 576 molecules model. Note that the metadynamics time does not correspond to real time.

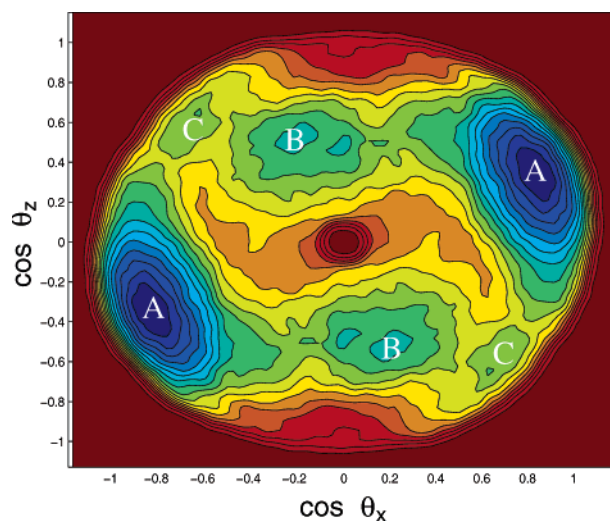


**Figure 2.** FES of ice  $I_h$  with respect to the orientation of the bond, which is being rotated to form the “5+7” defect at 120 K.

rings occur. These events correspond to the formation of 5+7 topological defects, which recombine after a short time. This defect was recently discovered by Grishina and Buch<sup>8</sup> and its five different conformations arising from the possible proton arrangements were analyzed.

The 5+7 defect can be viewed as originated from a double bond switching and a rotation of the O...O bond between the two water molecules displaced from their lattice sites. In a separate metadynamics run, we computed the free energy of the defect using as collective variables the orientation of the O...O bond with respect to two Cartesian axes,  $x$  and  $z$ . Simulations were performed in the NVT ensemble at two different temperatures, namely 120 and 270 K. The time-dependent potential is made up of the sum of Gaussians 0.167 kcal/mol high, placed every 1 ps, with  $\delta s = 0.03$  in both the dimensions of the collective variables space.

The FES obtained by metadynamics for the topological defect formation is represented in Figure 2. The FES displays a central symmetry, due to the fact that interchanging the two water molecules used to define the space of the collective variable has no effect on the energy of the system. Besides the two deep basins (labeled A in Figure 2) that correspond to the ideal crystal configuration, two inequivalent metastable structures have been identified (B and C in Figure 2). They both correspond to 5+7 defects, but the formation of five and seven-membered rings is achieved by different rotations of the pair of H<sub>2</sub>O molecules,

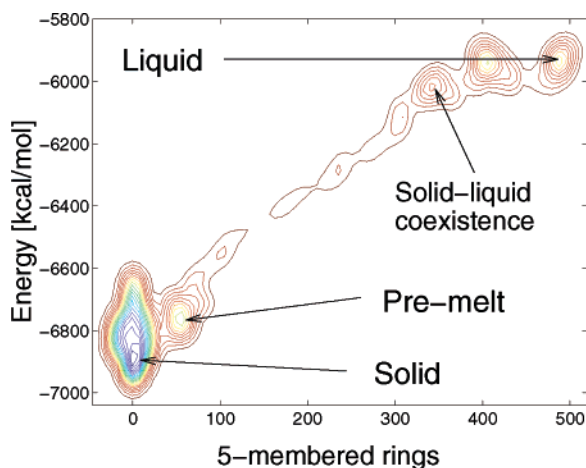


**Figure 3.** Two-dimensional projection of the FES into the space of the two collective variables energy and five-membered rings. The metadynamics run has been interrupted before the basin corresponding to the liquid state was explored.

leading to structures of varying stability, in agreement with the analysis of ref. 8. The free energy of the most stable defect structure (B) is 6.9 kcal/mol higher than that of the ideal crystal, which we assume as the reference zero value. The free energy barriers for the defect formation and recombination are estimated to be 8.9 and 2.0 kcal/mol, respectively, which, assuming a characteristic frequency for the reaction coordinates of  $\sim 5$  THz and using the classical transition state theory, gives an estimated lifetime of the defect of  $\sim 0.5$  ns at 120 K. The second defect structure (C) explored during the metadynamics run is less stable (8.4 kcal/mol) and can either recombine or transform into structure B through a barrier of 0.9 kcal/mol. When the temperature is raised to 270 K, the height of the free energy minimum corresponding to structure B and its formation and recombination barriers remain unchanged, whereas the recombination barrier for structure C goes to zero. These free energy calculations extend the results of ref 8 to finite temperature and confirm the relevance of these topological defects also at the melting temperature.

We found that the “5+7” defects play an even greater role, since they are responsible for the shallow minimum in the FES indicated as premelt in Figure 3. From metadynamics, the transition barrier to this local minimum can be estimated at roughly 12 kcal/mol. We analyzed the nature of this local minimum by performing an inherent structure analysis<sup>24</sup> of the metadynamics trajectory, quenching to zero K in 50 ps frames of the MD trajectory taken every 2 ps. As shown in Figure 4, the inherent structures display a relevant quantity of five-membered rings and a smaller number of four-membered rings and coordination defects. In fact these structures correspond to a condensation of topological defects involving about 50 H<sub>2</sub>O molecules in an otherwise perfect ice I<sub>h</sub> lattice. As the tetrahedral coordination is preserved, five-membered rings are accompanied by an equal number of seven-membered ones. One typical defect cluster thus obtained is shown in Figure 5. The energy of the particles, either belonging to smaller rings or under-coordinated, ranges from 0.60 to 0.95 kcal/mol relative to the energy of ice I<sub>h</sub>.

These defective structures were then embedded in a crystalline ice I<sub>h</sub> supercell containing 4608 molecules and brought to 270 K, to observe their stability. Several MD simulations were performed in the NPT ensemble with different random initial velocities. Remarkably, the average lifetime of the cluster of topological defects is  $0.4 \pm 0.1$  ns. This relatively stable

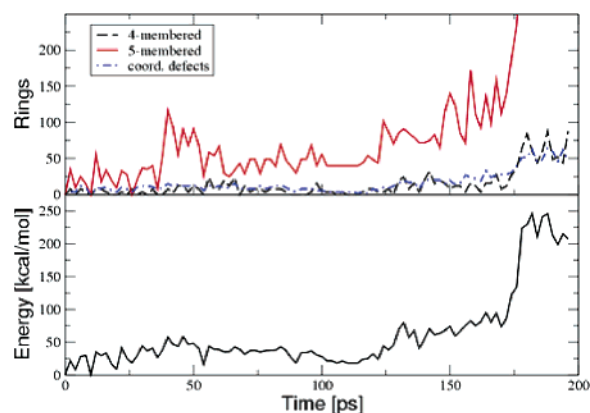


**Figure 4.** Defect statistics and energy of the inherent structures visited by the system in the premelt region. The zero of this graph corresponds to the beginning of the melting transition in a metadynamics run of a model with 576 water molecules.

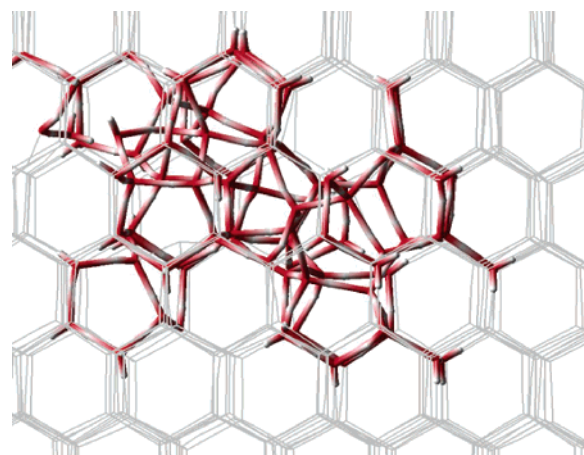


**Figure 5.** Cluster of topological defects obtained during the inherent structure analysis of the premelting phase. H<sub>2</sub>O molecules forming either four- or five-membered rings are represented by colored sticks. Grey lines represent the ice I<sub>h</sub> structure embedding the cluster of defects.

accumulation of defects in a restricted region of the crystal is a nucleus for further disorder and melting as the number of coordination defects and smaller rings grows. In Figure 4, two distinct regimes in the premelting inherent structures can be observed. When the system is dragged out of the free-energy basin corresponding to the cluster of topological defects, a relevant number of small rings and coordination defects appears and the energy suddenly increases. Roughly speaking, this signals the watershed between configurations belonging to the basin of attraction of ice I<sub>h</sub> and to that of the liquid.

Since the topological defects cannot migrate, the mobility of the defective droplet is related only to defect formation and recombination at the interface with the crystal, and no relevant motion of its center of mass was observed. We computed the momentum of inertia of the defective region and found that the inertia tensor has two eigenvalues  $I_1$  and  $I_2$  of similar size and a smaller one  $I_3$ , with an asphericity ratio  $(I_1 + I_2)/2 - I_3/(I_1 + I_2)/2 + I_3 \approx 0.4$ . This indicates that the cluster of defects has a somewhat elongated shape. The analysis of the eigenvectors shows that the defective region is roughly aligned along the  $(\bar{3}\bar{1}1)$  crystallographic direction.

Another feature of the FES that is worth commenting upon is the shallow basin that appears just before the larger liquid basin and corresponds to a liquid–solid interface.

In summary, our simulations reveal that topological defects where five- and seven-membered rings are formed play a crucial

role in the bulk melting of ice. It is worthy of note that in their landmark simulation of ice nucleation Matsumoto et al.<sup>25</sup> found that clusters with a similar structure to ours provide the nuclei for crystallization. The elongated shape of these extended defects and their preferential orientation along a given crystallographic direction might facilitate their experimental detection. Newly developed experimental techniques able to reveal inherent substructures in liquid water and in ice  $I_h$ <sup>26</sup> may provide direct evidence of the existence of the premelting structure found in our simulations. The recent report that the radiation-induced amorphization process in silicon proceeds via the formation and aggregation of “5+7” defects<sup>27</sup> leads us to believe that this is a general feature of disordering processes in tetrahedral networks.

**Acknowledgment.** We thank V. Buch for fruitful discussions and A. Laio for many useful suggestions, including the use of the potential energy as an order parameter, and for reading the manuscript.

## References and Notes

- (1) Makkonen, L. *J. Phys. Chem. B* **1997**, *101*, 6196.
- (2) Furukawa, Y.; Nada, H. *J. Phys. Chem. B* **1997**, *101*, 6167.
- (3) Mishima, O.; Calvert, L. D.; Whalley, E. *Nature* **1984**, *310*, 393.
- (4) Fecht, H. J. *Nature* **1992**, *356*, 133.
- (5) Laio, A.; Parrinello, M. *Procs. Natl. Acad. Sci. U.S.A.* **2002**, *99*, 20.
- (6) Iannuzzi, M.; Laio, A.; Parrinello, M. *Phys. Rev. Lett.* **2003**, *90*, 238302.
- (7) Laio, A.; Rodriguez-Forteza, A.; Gervasio, F. L.; Ceccarelli, M.; Parrinello, M. *J. Phys. Chem. B* **2005**, *109*, in press.
- (8) Grishina, N.; Buch, V. *J. Chem. Phys.* **2004**, *120*, 5217.
- (9) Ceccarelli, M.; Danelon, C.; Laio, A.; Parrinello, M. *Biophys. J.* **2004**, *87*, 58.
- (10) Iannuzzi, M.; Parrinello, M. *Phys. Rev. Lett.* **2004**, *93*, 025901.
- (11) Churakov, S. V.; Iannuzzi, M.; Parrinello, M. *J. Phys. Chem. B* **2004**, *108*, 11567.
- (12) Martonak, R.; Laio, A.; Parrinello, M. *Phys. Rev. Lett.* **2003**, *90*, 075503.
- (13) Micheletti, C.; Laio, A.; Parrinello, M. *Phys. Rev. Lett.* **2003**, *92*, 170601.
- (14) Steinhardt, P. J.; Nelson, D. R.; Ronchetti, M. *Phys. Rev. B* **1983**, *28*, 784.
- (15) Radhakrishnan, R.; Trout, B. L. *J. Am. Chem. Soc.* **2003**, *125*, 7743.
- (16) King, S. V. *Nature* **1967**, *213*, 1112.
- (17) Yuan, X. L.; Cormack, A. N. *Comput. Mater. Sci.* **2002**, *24*, 343.
- (18) The hydrogen bond function is defined as
 
$$f_{ij} = \frac{1 - \left(\frac{r_{ij} - C}{r_O}\right)^{10}}{1 - \left(\frac{r_{ij} - C}{r_O}\right)^{20}} \sum_k^H \frac{1 - \left(\frac{r_{ik} + r_{jk} - r_{ij}}{r_H}\right)^8}{1 - \left(\frac{r_{ik} + r_{jk} - r_{ij}}{r_H}\right)^{12}}$$
- with  $C = 2.7$  Å,  $r_O = 0.5$  Å and  $r_H = 0.6$  Å. The first term in the product is a function of the  $O_iO_j$  distance which is 1 at 2.7 Å and decays to 0 at 3.5 Å. The second term is one when the difference  $O_iH_k + O_jH_k - O_iO_j$  is zero and tends to zero when it exceeds 0.6 Å.
- (19) Raiteri, P.; Laio, A.; Parrinello, M. *Phys. Rev. Lett.* **2004**, *93*, 087801.
- (20) Buch, V.; Sandler, P.; Sadlej, J. *J. Phys. Chem. B* **1998**, *102*, 8641.
- (21) Mahoney, M. W.; Jorgensen, W. L. *J. Chem. Phys.* **2000**, *112*, 8910.
- (22) Lísál, M.; Kolafa, J.; Nezbeda, I. *J. Chem. Phys.* **2002**, *117*, 8892.
- (23) Mahoney, M. W.; Jorgensen, W. L. *J. Chem. Phys.* **2001**, *114*, 363.
- (24) Stillinger, F. H.; Weber, T. A. *Phys. Rev. A* **1982**, *25*, 978.
- (25) Matsumoto, M.; Saito, S.; Ohmine, I. *Nature* **2002**, *416*, 409.
- (26) Khoshtariya, D. E.; Zahl, A.; Dolidze, T. D.; Neubrand, A.; van Eldik, R. *J. Phys. Chem. B* **2004**, *108*, 14796.
- (27) Marques, L. A.; Pelaz, L.; Aboy, M.; Enriques, L.; Barbolla, J. *Phys. Rev. Lett.* **2003**, *91*, 135504.